Organometallic building blocks with amino-substituted cyclopentadienyl and boratabenzene ligands for the synthesis of heterometallic complexes and clusters†‡§

Nicolas Auvray,[a] Tushar S. Basu Baul,¶[b] Pierre Braunstein,*[a] Pierre Croizat,[a] Ulli Englert,[b] Gerhard E. Herberich[b] and Richard Welter[c]

Received 13th February 2006, Accepted 6th April 2006
First published as an Advance Article on the web 28th April 2006
DOI: 10.1039/b602106a

A comparative study of the reactivity of isolobal rhenium and molybdenum carbonylmetallates containing a borole, in $[Re(\eta^5\text{-}C_4H_4BPh)(CO)_3]^-$ (**2**), a boratanaphthalene, in $[Mo(\eta^5\text{-}2,4\text{-}MeC_9H_6BMe)(CO)_3]^-$ (**4a**) and $[Mo(\eta^5\text{-}2,4\text{-}MeC_9H_6BN\textit{i}\text{-}Pr_2)(CO)_3]^-$ (**4b**), a boratabenzene, in $[Mo(\eta^5\text{-}3,5\text{-}Me_2C_5H_3BN\textit{i}\text{-}Pr_2)(CO)_3]^-$ (**6**) or a dimethylaminocyclopentadienyl ligand, in $[Mo(\eta^5\text{-}C_5H_4NMe_2)(CO)_3]^-$ (**7**), toward palladium(II), gold(I), mercury(II) and platinum(II) complexes has allowed an evaluation of the role of these π-bonded ligands on the structures and unprecedented coordination modes observed in the resulting metal–metal bonded, heterometallic complexes. The new metallate **6** was reacted with $[AuCl(PPh_3)]$, and with 1 or 2 equiv. $HgCl_2$, which afforded the new heterodinuclear complexes $[Au\{Mo(\eta^5\text{-}3,5\text{-}Me_2C_5H_3BN\textit{i}\text{-}Pr_2)(CO)_3\}(PPh_3)]$ (*Mo–Au*) (**10**) and $[Hg\{Mo(\eta^5\text{-}3,5\text{-}Me_2C_5H_3BN\textit{i}\text{-}Pr_2)(CO)_3\}Cl]$ (*Hg–Mo*) (**11**) and the heterometallic chain complex $[Hg\{Mo(\eta^5\text{-}3,5\text{-}Me_2C_5H_3BN\textit{i}\text{-}Pr_2)(CO)_3\}_2]$ (*Mo–Hg–Mo*) (**12**), respectively. Reactions of the new metallate **7** with $HgCl_2$, *trans*-$[PtCl_2(CN\textit{t}\text{-}Bu)_2]$ and *trans*-$[PtCl_2(NCPh)_2]$ yielded the heterodinuclear complex $[Hg\{Mo(\eta^5\text{-}C_5H_4NMe_2)(CO)_3\}Cl]$ (*Mo–Hg*) (**15**), the heterotrinuclear chain complexes *trans*-$[Pt\{Mo(\eta^5\text{-}C_5H_4NMe_2)(CO)_3\}_2(CN\textit{t}\text{-}Bu)_2]$ (*Mo–Pt–Mo*) (**16**) and *trans*-$[Pt\{Mo(\eta^5\text{-}C_5H_4NMe_2)(CO)_3\}_2(NCPh)_2]$ (*Mo–Pt–Mo*) (**17**), the mononuclear complex $[Mo(\eta^5\text{-}C_5H_4NMe_2)(CO)_3Cl]$ (**18**), the lozenge-type cluster $[Mo_2Pt_2(\eta^5\text{-}C_5H_4NMe_2)_2(CO)_8]$ (**19**) and the heterodinuclear complex $[Pt\{Mo(\eta^5\text{-}C_5H_4NMe_2)(CO)_3\}(NCPh)Cl]$(*Mo–Pt*) (**20**), respectively. The complexes **11**, **16**, **17**·2THF, **18** and **20** have been structurally characterized by X-ray diffraction and **20** differs from all other compounds in that the dimethylaminocyclopentadienyl ligand forms a bridge between the metals.

Introduction

The first borole-containing mixed-metal cluster, $[Re_2Pd_2(\eta^5\text{-}C_4H_4BPh)_2(CO)_6]$ (**1**), has been obtained by reaction of $[PdCl_2(COD)]$, *trans*-$[PdCl_2(NCPh)_2]$ or $[Pd_4(OAc)_4(CO)_4]$ with $[Re(\eta^5\text{-}C_4H_4BPh)(CO)_3]^-$ (**2**).[1] It has a planar, triangulated metal core and its cluster valence electron count (CVE) of only 54 contrasts with that of the planar, triangulated clusters $[M_2Pd_2(\eta^5\text{-}C_5H_5)_2(CO)_6(PEt_3)_2]$ (**3a–c**, M = Cr, Mo, W) which contain 58 CVE.[2]

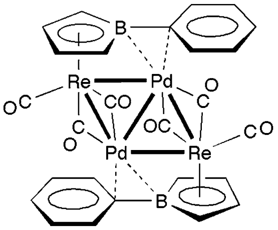

1

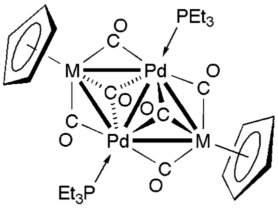

3a M = Cr
3b M = Mo
3c M = W

This unusual Re_2Pd_2 cluster displayed a unique bonding mode of the borole ligand which not only binds to rhenium in the usual η^5 manner but also to the adjacent palladium *via* a 2e–3c $B\text{–}C_{ipso}\text{–}Pd$ system. This led us to extend our studies on borole-containing carbonylmetallates to the 2-boratanaphthalene systems **4a**,**b**.[3] Their boron-containing six-membered aromatic ring should behave as a *neutral* five-electron donor, like the five-membered Cp ligand and the *anionic*, five-membered, borole ligand.

Consistently, the first metal cluster with a boratanaphthalene ligand, $[Mo_2Pd_2(\eta^5\text{-}2,4\text{-}MeC_9H_6BMe)_2(CO)_6(PEt_3)_2]$ (**5**), was prepared from **4a** and showed a planar, triangulated metal core with a centre of symmetry in the middle of the Pd–Pd bond, similar to that in the Cp derivatives **3**.[3]

---

[a] *Laboratoire de Chimie de Coordination, UMR 7177 CNRS, Université Louis Pasteur, 67070, Strasbourg Cédex, France. E-mail: braunst@chimie.u-strasbg.fr*
[b] *Institut für Anorganische Chemie der Rheinisch-Westfälischen Technischen Hochschule Aachen, Landoltweg 1, 52074, Aachen, Germany*
[c] *Laboratoire DECOMET, UMR 7177 CNRS, Université Louis Pasteur, 67070, Strasbourg Cédex, France*

† Electronic supplementary information (ESI) available: ORTEP views of a pair of molecules of **11** (Fig. S1) and views of the packing of molecules of **11** (Fig. S2). See DOI: 10.1039/b602106a

‡ Part of the PhD Thesis of P. C.

§ Dedicated to Prof. P. Zanello on the occasion of his 65th birthday, with our warmest wishes.

¶ Present address: Department of Chemistry, North-Eastern Hill University, NEHU Permanent Campus, Umshing, Shillong 793 022, India.

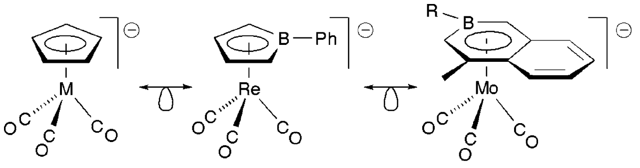

M = Cr, Mo, W **2** **4a** R = Me **4b** R = N*i*-Pr$_2$

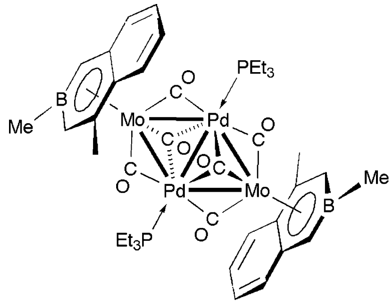

5

Intrigued by the 2e–3c B–C$_{ipso}$–Pd bonding in cluster **1**, we wondered whether a stronger donor substituent than the *ipso* carbon of the phenyl group of **2**, such as an amino group, would be able to interact with the adjacent metal and confer more stability to the product. In heterodinuclear Ag–Mo, Au–Mo and Hg–Mo complexes prepared from the boratanaphthalene tricarbonylmolybdate **4b**, no interaction was found between the amino group and the metal adjacent to the molybdenum centre.[3] We decided to compare the reactivity and bonding in heterometallic complexes of three related tricarbonylmolybdates: the new diisopropylamino-boron-substituted 3,5-dimethylboratabenzene derivative [Mo(η^5-3,5-$Me_2C_5H_3BN$*i*-Pr_2)$(CO)_3$]$^-$ (**6**), the 2-diisopropylamino-4-methyl-2-boratanaphthalene analogue [Mo(η^5-2,4-$Me_2C_9H_6BN$-*i*-Pr_2)$(CO)_3$]$^-$ (**4b**)[3] and the new amino-substituted cyclopentadienyltricarbonylmolybdate [Mo(η^5-$C_5H_4NMe_2$)$(CO)_3$]$^-$ (**7**).

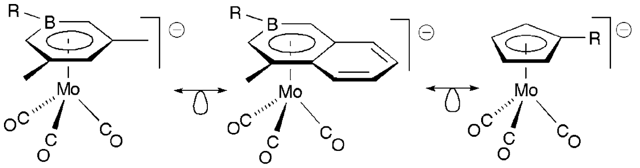

6 R = N*i*-Pr$_2$ **4a** R = Me **4b** R = N*i*-Pr$_2$ **7** R = NMe$_2$

Borabenzene **8** does not exist due to a low-lying in plane σ*-type LUMO which is essentially localized at the boron atom.[4,5] Therefore stabilization by a Lewis base is necessary and is achieved in the amino-substituted boratabenzene **9**.[6,7]

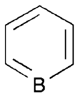

8

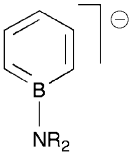

9

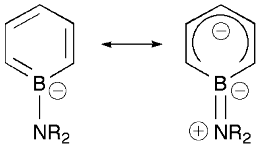

The first boratabenzene complex was obtained in 1970 from a cobaltocene[8] while Li(TMPA)($C_5H_5BNMe_2$) (TMPA = $Me_2N(CH_2)_3NMe_2$) was, in 1993, the first boratabenzene salt structurally characterized.[6] The presence of a lone pair on the nitrogen of the dialkyl amino group results in a partial double bond between the boron and nitrogen atoms.[6,7,9,10]

Results and discussion

1 Boratabenzene complexes

The 1,2-dimethoxyethane (DME)-solvated lithium salt of the 1-diisopropylamino-3,5-dimethylboratabenzene tricarbonylmolybdate [Mo(η^5-3,5-$Me_2C_5H_3BN$*i*-Pr_2)$(CO)_3$]$^-$ (**6**) was prepared by reaction between Li(3,5-$Me_2C_5H_3BN$*i*-Pr_2)[11] and [Mo$(CO)_6$] (see Experimental section). It was reacted with [AuCl(PPh_3)] to afford the heterodinuclear complex **10**, which is analogous to the known Cp[12,13] or substituted Cp derivative C_5H_4CHO[14] and boratanaphthalene Au–Mo complexes.[3]

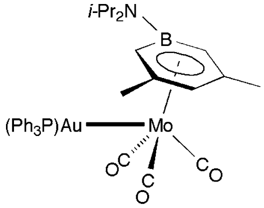

10

When Li·**6**·2DME was reacted with $HgCl_2$ in a 1 : 1 ratio, the heterodinuclear complex **11** was obtained, of which the structure was determined by X-ray diffraction. One of the two independent molecules of similar conformation is represented in Fig. 1(a); the caption provides a comparison of relevant interatomic distances and angles in both molecules. An ORTEP view of the complete asymmetric unit is available in Fig. S1 (ESI†). The four-legged piano stool-type geometry around the molybdenum atom, defined by the three carbonyl groups and the mercury atom, is similar to that observed in [Hg{Mo(η^5-C_5H_5)$(CO)_3$}Cl][15,16] and [Mo(η^5-C_5H_5)$(CO)_3$Cl].[16] The Hg–Mo distance of 2.6904(16) Å [2.6852(15) Å in the second molecule] is very similar to that observed in [Hg{Mo(η^5-C_5H_5)$(CO)_3$}Cl] (2.683(1) Å).[16] The boron atom is situated 0.3244(2) Å [0.3322(2) Å] out of the mean plane defined by the carbon atoms of the boratabenzene ring. Thus, the bonding mode of the heterocycle to the molybdenum atom is closer to η^5 than η^6. The B–N double-bond character is reflected in the distance of 1.406(18) [1.453(17)] Å[17] and the sum of the angles around N is 359.6(12) [360.0(11)]°. These features are similar to those encountered in a related Au–Mo complex.[3] A torsional orientation of the ring brings the amino group connected to the boron atom at a N ··· Hg distance of 3.561(10) Å

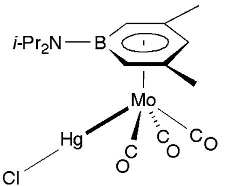

11

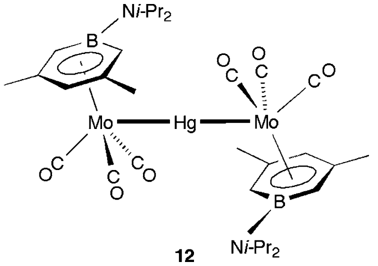

12

[3.584(10) Å], which is too long to represent a significant bonding interaction. The Cl–Hg–Mo angle is 177.82(11)° [173.69(12)°] and intermolecular interactions between the mercury and the chlorine atoms of two proximate molecules in the unit cell result in Hg · · · Cl separations of 3.483(5) and 3.430(5) Å (Fig. 1(b)). A view of the solid-state packing is shown in Fig. S2 (ESI†).

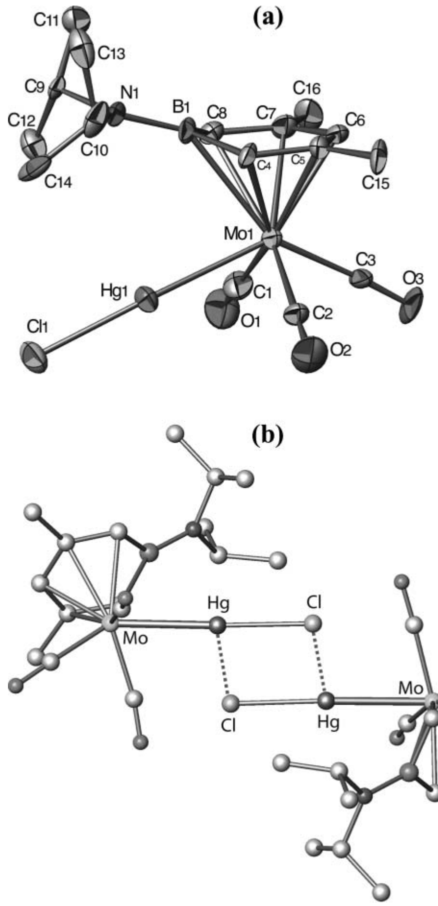

Fig. 1 (a) ORTEP view of one of two independent molecules in the structure **11** with the atom-numbering scheme. Displacement ellipsoids enclose 50% of the electron density. Selected bond distances (Å) and angles (°) [values for the second molecule in square brackets]: Hg(1)–Mo(1) 2.6904(16) [2.6852(15)], Hg(1)–Cl(1) 2.404(4) [2.397(4)], Mo(1)–C(1) 1.995(14) [2.032(15)], Mo(1)–C(2) 2.013(15) [1.989(15)], Mo(1)–C(3) 1.944(14) [1.972(14)], C(1)–O(1) 1.141(14) [1.121(15)], C(2)–O(2) 1.130(15) [1.150(15)], C(3)–O(3) 1.169(15) [1.154(15)], B(1)–N(1) 1.406(18) [1.453(17)]; Mo(1)–Hg(1)–Cl(1) 177.84(11) [173.72(11)], Mo(1)–C(1)–O(1) 175.9(13) [178.1(14)], Mo(1)–C(2)–O(2) 171.8(14) [174.5(14)], Mo(1)–C(3)–O(3) 179.4(14) [176.3(14)], C(1)–Mo(1)–Hg(1) 79.9(4) [75.0(4)], Hg(1)–Mo(1)–C(2) 72.0(4) [74.5(4)], C(2)–Mo(1)–C(3) 77.9(6) [77.8(6)], C(3)–Mo(1)–C(1) 79.2(6) [77.9(6)], C(1)–Mo–C(2) 104.3(6) [109.2(6)], B(1)–N(1)–C(9) 125.1(11) [123.2(11)], B(1)–N(1)–C(10) 119.8(11) [123.4(11)], C(9)–N(1)–C(10) 114.7(10) [113.4(10)]. (b) View of the intermolecular interactions between molecules of **11**. Hg · · · Cl = 3.483(5) and 3.430(5) Å.

When Li·**6**·2DME and $HgCl_2$ were reacted in a 2 : 1 ratio, the expected heterotrinuclear complex **12** was obtained. In the related centrosymmetric *N*-diisopropylamino-2-boratanaphthalene derivative **13** an exo-type orientation of the amino groups was established by X-ray diffraction.[3] In contrast, the neutral silver analog **14**, which contains one protonated amino group (*i.e.* one B-amino and one B-ammonio substituent), showed a different, endo-type orientation of the 2-boratanaphthalene ligands, however with no significant interaction between the amino-N and Ag atoms (4.617(2) Å).[3]

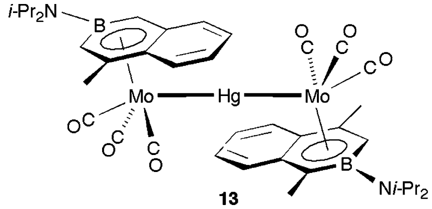

13

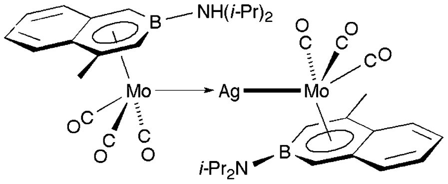

14

With the amino-substituted boratabenzene or boratanaphthalene systems described so far, no bonding interaction between the nitrogen atom and a metal centre was observed. We have then turned our attention to amino-substituted Cp derivatives, related to the phenylborole ligand present in cluster **1**.

2 Amino-Cp complexes

We first prepared the new metallate Li[Mo(η^5-$C_5H_4NMe_2$)$(CO)_3$]·2DME (Li·**7**·2DME) by reaction of Li($C_5H_4NMe_2$)[18] with [Mo$(CO)_6$] in refluxing DME, by analogy with the synthesis of Na(C_5H_5)·DME (see Experimental section).[19] Its reaction with $HgCl_2$ in a 1 : 1 ratio was carried out with the objective to structurally characterize the expected Mo–Hg–Cl product [Hg{Mo(η^5-$C_5H_4NMe_2$)$(CO)_3$}Cl] (**15**). However, the crystals obtained were not of good enough quality to allow a complete structural resolution but the N · · · Hg separation found of *ca.* 3.5 Å is analogous to that observed in **11** (see Experimental section).

The synthesis of linear Mo–Pt–Mo complexes was envisaged in order to answer the question of a possible coordination of the Cp-bound amino group to platinum. The reaction between Li·**7**·2DME and *trans*-[$PtCl_2(CNt\text{-}Bu)_2$] in a 2 : 1 ratio was performed in THF at −40 °C. It afforded the expected trinuclear complex *trans*-[Pt{Mo(η^5-$C_5H_4NMe_2$)$(CO)_3$}$_2$(CN*t*-Bu)$_2$] (**16**) as an orange compound, analogous to the parent Cp derivative.[20] Its structure determination by X-ray diffraction showed that the Pt atom lies on an inversion centre. An ORTEP view is shown in Fig. 2 with the main distances and angles. The four-legged piano stool type geometry around the molybdenum atoms, defined by the three

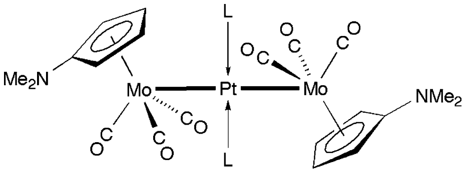

16 L = CN*t*-Bu
17 L = NCPh

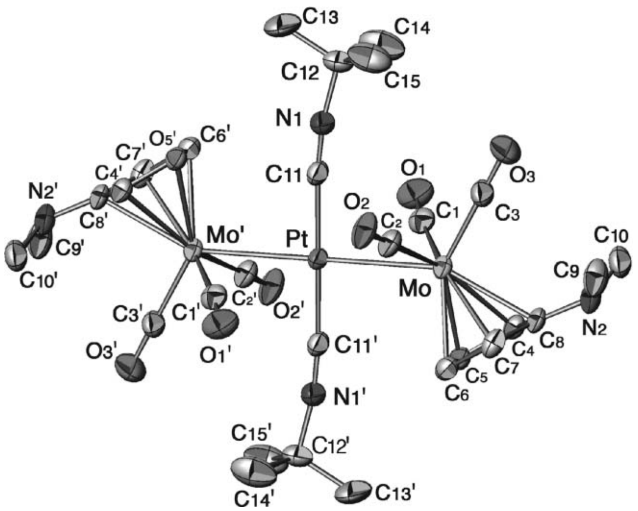

Fig. 2 ORTEP view of the structure **16** with the atom-numbering scheme. Operators for generating equivalent, primed atoms ($-x$, $-y$, $-z$). Displacement ellipsoids enclose 50% of the electron density. Selected bond distances (Å) and angles (°): Pt–Mo 2.868(1), Pt–C(11) 1.958(6), Mo–C(1) 1.976(6), Mo–C(2) 1.983(6), Mo–C(3) 1.953(6), C(1)–O(1) 1.156(7), C(2)–O(2) 1.156(7), C(3)–O(3) 1.150(7), C(8)–N(2) 1.376(6); Mo–C(1)–O(1) 173.4(5), Mo–C(2)–O(2) 172.4(5), Mo–C(3)–O(3) 179.7(6), Mo–Pt–C(11)' 87.6(1), Mo–Pt–C(11) 92.4 (2), Pt–Mo–C(1) 65.5(2), C(1)–Mo–C(3) 81.0(3), C(3)–Mo–C(2) 82.2(3), C(2)–Mo–Pt 61.8(2), C(2)–Mo–C(1) 108.8(2), C(8)–N(2)–C(9) 115.6(5), C(8)–N(2)–C(10) 116.1(5), C(9)–N(2)–C(10) 115.8(5).

carbonyl groups and the platinum atom, is similar to that observed in **11** and [Mo(η^5-C_5H_5)(CO)$_3$Cl].[16] However, in contrast to **11**, the crystal structure of **16** reveals an exo-type orientation of the amino groups, most probably because of the presence of the bulky *t*-BuNC ligands coordinated to the platinum. The carbonyl groups on each Mo(η^5-$C_5H_4NMe_2$)(CO)$_3$ fragment are quasi terminal, the Mo–C(1)–O(1), Mo–C(2)–O(2) and Mo–C(3)–O(3) angles being of 173.4(5), 172.4(5) and 179.7(6)°, respectively. The C(1)–Pt (2.725(5) Å) and C(2)–Pt (2.604(7) Å) separations appear to be too long to represent a significant bonding interaction. However, when considering the structural asymmetry parameter $a = (d_2 - d_1)/d_2$ (Scheme 1) often used to characterize the bonding situation of carbonyl ligands,[21] its value for the ligands C(1)O(1) and C(2)O(2) of 0.38 and 0.31, respectively, could qualify them for being semi-bridging.

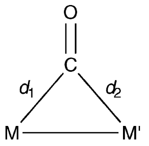

Scheme 1 $a = (d_2 - d_1)/d_1$; $0.1 \leq a \leq 0.6$: semi bridging carbonyl; $a \leq 0.1$: bridging carbonyl; $a \geq 0.6$: terminal carbonyl.

The platinum coordination plane and the C_5 ring are orthogonal to each other (90.0(2)°). In contrast to the situation in **11**, the nitrogen atoms connected to the Cp rings are in a pyramidal environment (sum of the angles around N of 348(2)°), and this is consistent with a pure σ-bond between the nitrogen and the Cp ring.

With the hope of generating a 2e–3c C_{ipsoCp}–N–Pt interaction or a 2e–2c N–Pt bond, we reacted Li·**7**·2DME with *trans*-[PtCl$_2$(NCPh)$_2$], which contains labile PhCN ligands, in a manner similar to that described for *trans*-[PtCl$_2$(CN*t*-Bu)$_2$]. The major compound obtained in this reaction was *trans*-[Pt{Mo(η^5-$C_5H_4NMe_2$)(CO)$_3$}$_2$(NCPh)$_2$] (*Mo–Pt–Mo*) (**17**). The X-ray diffraction analysis of **17**·2THF established that the Pt atom lies on an inversion centre and the resulting linear arrangement of the metals is also found in related Cp complexes.[22,23] There is no C_{ipsoCp}–N–Pt interaction. An ORTEP view is shown in Fig. 3 with the main distances and angles. Despite its much higher lability compared to *t*-BuNC, the benzonitrile ligand is obviously not displaced by the NMe_2 donor group.

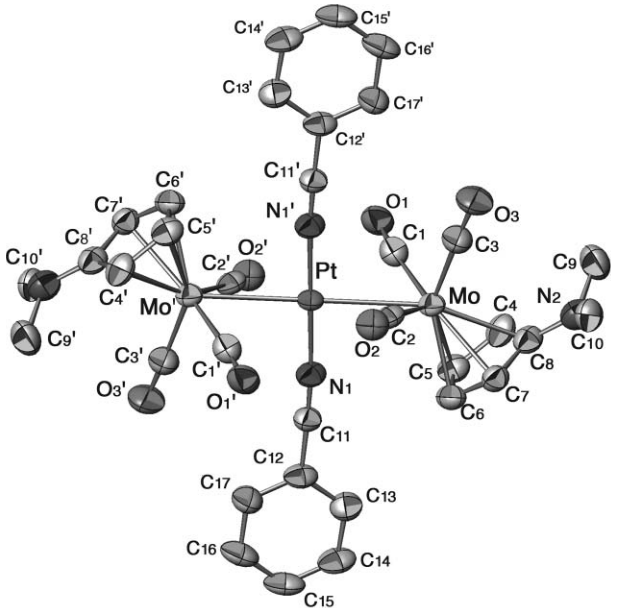

Fig. 3 ORTEP view of the structure **17** in **17**·2THF with the atom-numbering scheme. Operators for generating equivalent, primed atoms ($-x$, $-y$, $1 - z$). Displacement ellipsoids enclose 50% of the electron density. Selected bond distances (Å) and angles (°): Pt–Mo 2.854(3), Pt–N(1) 1.942(7), Mo–C(1) 1.98 (1), Mo–C(2) 1.97(1), Mo–C(3) 1.93(1), C(1)–O(1) 1.16(1), C(2)–O(2) 1.16(1), C(3)–O(3) 1.18(1), C(8)–N(2) 1.36(1); Mo–C(1)–O(1) 172.0(9), Mo–C(2)–O(2) 170.1(8), Mo–C(3)–O(3) 177(1), Mo–Pt–N(1) 92.9(2), Mo–Pt–N(1)' 87.1(2), Pt–Mo–C(1) 62.3(3), C(1)–Mo–C(3) 85.3(4), C(3)–Mo–C(2) 82.0(4), C(2)–Mo–Pt 59.4(3), C(2)–Mo–C(1) 113.4(3), C(8)–N(2)–C(9) 119.9(9), C(8)–N(2)–C(10) 116.7(9), C(9)–N(2)–C(10) 111.9(9).

The crystal structure of **17** is very similar to that of **16** and the Mo–Pt distances are almost the same (2.854(3) Å for **17**, 2.868(1) Å for **16**). The orientation of the amino-Cp ring with respect to the platinum coordination plane is 85.8(4)°. The sum of the angles around the nitrogen atom of the NMe_2 groups N(2) is 349(3)°. The carbonyl groups of the Mo(η^5-$C_5H_4NMe_2$)(CO)$_3$ fragment are almost terminal, with Mo–C(1)–O(1), Mo–C(2)–O(2) and Mo–C(3)–O(3) angles very similar to their analogues in **16**. The Pt–C(1) and Pt–C(2) distances in **17** (2.61(1) Å and 2.509(9) Å) are slightly shorter than in **16** (2.725(5) and 2.604(7) Å, respectively). Considering the values of the parameter $a = (d_2 - d_1)/d_2$ (Scheme 1) for the ligands C(1)O(1) and C(2)O(2) of 0.32

and 0.27, respectively, these ligands may also be considered as semi-bridging.[21,24–26]

Three other compounds which are soluble in diethyl ether were also obtained in low yields from the reaction leading to **17**. The most soluble of them, even in pentane, was characterized by X-ray diffraction as the mononuclear complex [Mo(η^5-$C_5H_4NMe_2$)$(CO)_3Cl$] (**18**).An ORTEP view is shown in Fig. 4 with the main distances and angles. This four legged piano stool structure and the bond distances and angles are very similar to those in [Mo(η^5-C_5H_5)$(CO)_3Cl$].[16] The nitrogen atom is in an almost perfectly planar environment (the sum of the angles around N is 359.0(9)°). This complex obviously results from a redox reaction. The red–brown, 58 CVE cluster [Mo_2Pt_2(η^5-$C_5H_4NMe_2)_2(CO)_8$] (**19**) was also isolated by fractional crystallization, and its crystal structure showing a metal core similar to that in the clusters **3b** and in [Mo_2Pt_2(η^5-$C_5H_5)_2(CO)_6(PEt_3)_2$][22] will be detailed elsewhere.

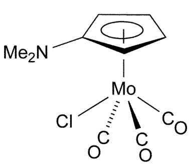

18

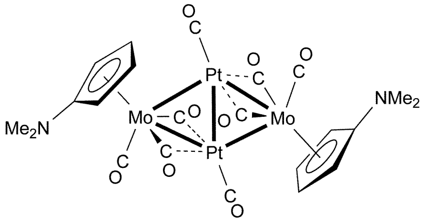

19

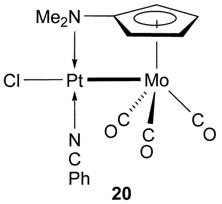

20

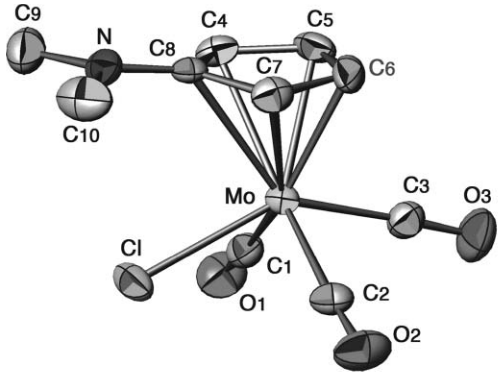

Fig. 4 ORTEP view of the structure **18** with the atom-numbering scheme. Displacement ellipsoids enclose 50% of the electron density. Selected bond distances (Å) and angles (°): Mo–Cl 2.518(1), Mo–C(1) 1.995(3), Mo–C(3) 1.987(3), Mo–C(2) 2.030(3), C(1)–O(1) 1.142(4), C(3)–O(3) 1.138(4), C(2)–O(2) 1.138(3), C(8)–N 1.327(4); Mo–C(1)–O(1) 174.5(2), Mo–C(3)–O(3) 177.4(3), Mo–C(2)–O(2) 176.1(3), Cl–Mo–C(1) 80.6(1), C(1)–Mo–C(3) 79.3(1), C(2)–Mo–C(3) 79.4(1), C(2)–Mo–Cl 77.83(9), C(1)–Mo–C(2) 111.1(1), C(8)–N–C(9) 120.4(3), C(8)–N–C(10) 120.5(3), C(9)–N–C(10) 118.1(3).

A more unexpected molecule was the pale orange heterodimetallic complex [Pt{Mo(η^5-$C_5H_4NMe_2$)$(CO)_3$}(NCPh)Cl] (*Mo–Pt*) (**20**) which was shown by X-ray diffraction to display a bonding interaction between the amino donor function of the cyclopentadienyl ring and the platinum centre. An ORTEP view is shown in Fig. 5 with the main distances and angles. The Pt–Mo distance of 2.748(1) Å is slighly shorter than in **16** (2.868(1) Å) and **17** (2.854(3) Å). The Pt–N(2) distance is 2.079(5) Å and the non-planar environment of this nitrogen atom (sum of the angles around N(2) of 332(2)°), confirms its coordination to platinum. This results in a lengthening of the N(2)–C(8) bond (1.455(9) Å) compared to its value in **17** (1.36(1) Å). Although only a unique crystal of this complex was obtained, despite attempts to prepare or isolate it in larger quantities, which precluded recording of spectroscopic data, we believe that its interesting structure warrants a mention since this appears to be the first example of such an intramolecular bridging coordination mode for an amino-cyclopentadienyl ligand. It is however related to that in phosphino-cyclopentadienyl heterometallic systems.[27,28]

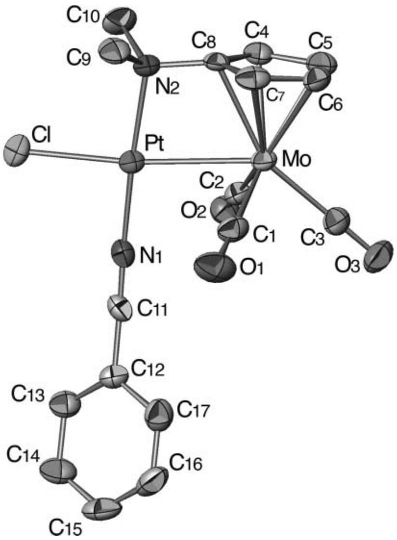

Fig. 5 ORTEP view of the structure **20** with the atom-numbering scheme. Displacement ellipsoids enclose 50% of the electron density. Selected bond distances (Å) and angles (°): Pt–Mo 2.748(1), Pt–Cl 2.401(2), Pt–N(1) 1.956(6), Pt–N(2) 2.079(5), Mo–C(1) 1.967(8), Mo–C(2) 1.983(7), Mo–C(3) 1.995(8), C(1)–O(1) 1.159(9), C(2)–O(2) 1.157(8), C(3)–O(3) 1.155(8), C(8)–N(2) 1.455(9); Mo–Pt–N(1) 96.9(2), Mo–Pt–N(2) 79.8(2), N(2)–Pt–Cl 93.4(2), N(1)–Pt–Cl 89.8(2), Mo–C(1)–O(1) 176.2(7), Mo–C(2)–O(2) 175.1(6), Mo–C(3)–O(3) 178.6(7), Pt–N(2)–C(9) 109.9(4), Pt–N(2)–C(10) 112.1(4), Pt–N(2)–C(8) 102.6(4), Pt–Mo–C(2) 70.3(2), C(2)–Mo–C(3) 81.2(3), C(3)–Mo–C(1) 83.1(3), C(1)–Mo–Pt 72.8(2), C(1)–Mo–C(2) 101.4(3), C(8)–N(2)–C(9) 112.3(5), C(8)–N(2)–C(10) 112.8(5), C(9)–N(2)–C(10) 107.3(6).

The fact that this dinuclear complex could be isolated indicates that substitution of the second chloride leading to **17** is slow enough to allow the η^5-C_5H_4-bound NMe_2 group to irreversibly displace one of the Pt-bound benzonitrile ligands (Scheme 2).

Because of the too small quantity of complex **20** isolated, we could not yet verify that it would react with another equivalent of **7** to give, logically, a Mo–Pt–Mo chain complex with two bridging amino-cyclopentadienyl ligands, similar to a Mo–Pd–Mo complex containing two bridging phosphino-cyclopentadienyl ligands.[28]

From a structural view point, it appeared interesting to compare the coordination geometry about the Mo centre in the different complexes structurally analyzed in this work by using as parameters the angles between the mean plane formed by the carbon atoms of the π-ligand and the plane defined by the carbon atoms

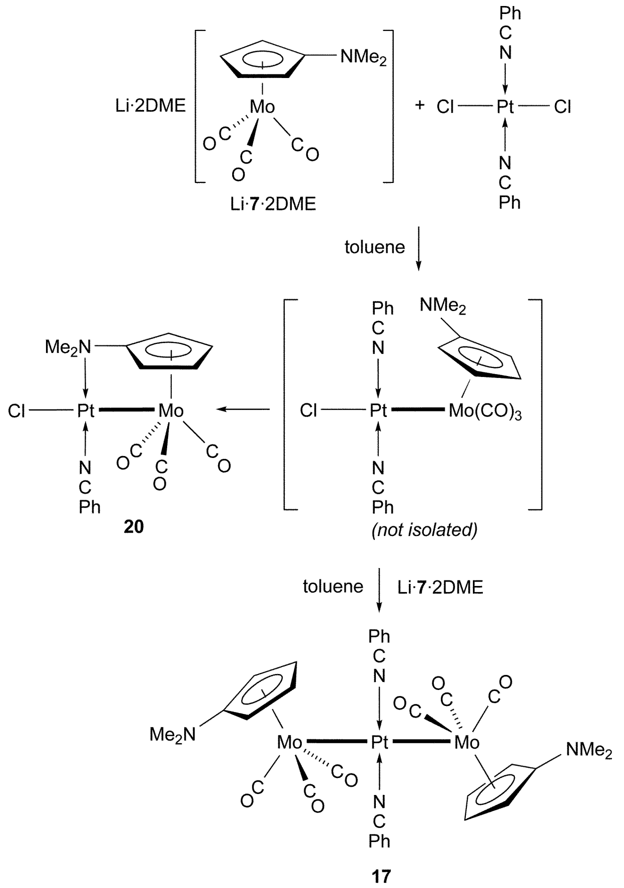

Scheme 2 Suggested mechanism for the formation of complexes **17** and **20**.

of the three carbonyl ligands (angle *β*) and that between the mean plane formed by the carbon atoms of the π-ligand and the mean plane defined by these three carbon atoms and the fourth substituent X (angle *γ*) (Table 1).

A typical four-legged piano-stool structure is characterized by very small values of the *γ* angle. As an example, this is the case in the very regular four-legged piano-stool structure of [Ta(η^5-C_5H_5)$(CO)_4$], with a *γ* angle of 1.32(1)°.[29] In the case of **18**, in which the Mo–X and Mo–CO distances are much closer than in the other complexes studied, the low value of *γ* is consistent with a four-legged piano stool structure. A typical, regular three-legged piano-stool structure is characterized by a very small β angle, as in [Mo(η^5-C_5H_5)$(CO)_3$]$^-$ (1.95(1)°).[30]

In complex **20**, the angle *γ* is 11.56(2)° and the geometry about the Mo atom becomes better described as a three-legged piano-stool with the X ligand (here Pt) capping a face of the MoC_3 tetrahedron. In this case, it is the *β* angle which becomes very small (1.19(2)°). Consistently, the Mo–X distance increases compared to that in **18**.

However, since the orientation of the mean plane defined by C(1), C(2), C(3) and the fourth leg X of the piano stool with respect to the π-bonded ring also depends on the difference between the Mo–X and Mo–CO distances, the parameter *γ* may not always be ideal for making valid comparisons. Therefore, we also provide in Table 1 a comparison of the angles between the *trans* ligands C(1)–Mo–C(2) and C(3)–Mo–X. We also compare the angles between the Mo–CO or Mo–X bonds and the axis passing through the molybdenum and the π-bonded ring centroid. These values confirm that the most regular four-legged piano stool structure is that of **16**. In the case of **20** the three centroid–Mo–C angles are almost equal, whereas the centroid–Mo–X (Pt in this case) is much smaller, consistent with the description of a three-legged piano stool structure with one MoC_3 face capped by X. For **11**, **17** and **18**, these parameters indicate an intermediate situation and irregular four-legged piano stool structures.[16]

Conclusion

In this work, we have examined the reactivity of a set of isolobal organometallic building blocks toward metal complexes with a d^8 (Pd(II), Pt(II)) or d^{10} (Au(I), Hg(II)) electronic configuration with the aim to synthesize metal–metal bonded heterometallic complexes. We have shown that the tricarbonylmolybdates **4a**,**b**, **6** and **7**, which contain boratanaphthalene, boratabenzene and cyclopentadienyl π-bonded ligands, respectively, all have a metal-centred nucleophilicity which explains the formation of the metal–metal bonded products. The amino function bonded to the boron atom in **4b** and **6** did not participate in direct bonding to a metal adjacent to the Mo atom. In contrast, the amino-substituted cyclopentadienyl ligand in **7** can support a metal–metal bond, as observed in the Mo–Pt complex **20**.

Table 1 Comparison of the structural parameters in complexes of the type [Mo(η^5-C_5H_5)$(CO)_3$X]

Angle/°	[TaCp$(CO)_4$]	[MoCp$(CO)_3$]$^-$	**11** (mol. 1)	**11** (mol. 2)	**16**	**17**·2THF	**18**	**20**
β[a]	—	1.95(1)	12.5(8)	6.2(8)	1.17(2)	4.34(2)	19.89(1)	1.19(2)
γ[b]	1.32(1)	—	1.1(7)	1.2(7)	6.20(2)	9.41(2)	7.74(1)	11.56(2)
C(1)–Mo–C(2)	117.4(3)	—	104.2(6)	109.2(6)	108.8(2)	113.4(3)	111.1(1)	101.4(3)
C(3)–Mo–X	117.4(3)	—	137.5(5)	131.7(4)	115.8(2)	105.7(3)	141.6(1)	137.5(2)
Centroid–Mo–C(1)	122.0(2)	127.24(1)	126.3(5)	125.3(5)	124.0(2)	120.1(3)	122.07(8)	126.8(2)
Centroid–Mo–C(2)	122.0(2)	127.63(1)	128.5(5)	124.6(5)	124.5(2)	121.4(3)	126.76(9)	124.8(2)
Centroid–Mo–C(3)	120.6(2)	125.01(1)	117.3(5)	120.0(5)	119.5(2)	122.9(3)	111.1(1)	125.1(2)
Centroid–Mo–X	120.6(2)	—	104.95(3)	108.26(4)	124.74(2)	131.43(4)	107.3(2)	97.19(3)

[a] *β*: angle between the mean plane defined by the carbon atoms of the π-bonded ring (Cp or boratabenzene) and the plane defined by the C(1), C(2), C(3) atoms. [b] *γ*: angle between the mean plane defined by the carbon atoms of the π-bonded ring (Cp or boratabenzene) and the mean plane defined by C(1), C(2), C(3) and the fourth leg X of the piano stool (X = Hg, Pt or Cl).

Experimental

General procedures

Reactions were carried out under an atmosphere of nitrogen by means of conventional Schlenk techniques. Hexane was distilled from sodium/potassium alloy, toluene from sodium, diethyl ether from sodium/benzophenone, and dichloromethane from calcium dihydride. When indicated, melting points were determined in sealed capillaries on a Büchi 510 melting point apparatus and are uncorrected. Elemental analyses were performed by Analystische Laboratorien, Prof. Dr. H. Malissa and G. Reuter GmbH, D-51789 Lindlar, Germany and by the "Service de Microanalyses", Université Louis Pasteur, Strasbourg.

NMR spectra were recorded on a Varian Unity 500 (^{1}H, 500 MHz; ^{13}C, 125.7 MHz; ^{11}B, 160.4 MHz; ^{31}P, 202.4 MHz), a Varian VXR 300 or Bruker Avance 300 (^{1}H, 300 MHz; ^{13}C, 75.47 MHz; ^{31}P, 121.49 MHz) or a Varian Mercury 200 (^{1}H, 200 MHz) spectrometer. Chemical shifts (in ppm) were measured at ambient temperature and are referenced to internal TMS for ^{1}H and ^{13}C and to external $BF_3{\cdot}OEt_2$ for ^{11}B, and external H_3PO_4 (84%) for ^{31}P, with downfield shifts reported as positive. The spectra were measured at 298 K. Deuterated solvents for NMR spectroscopy were degassed, dried and stored over molecular sieves (4 Å Merck). Assignments are based on APT and DEPT spectra and ^{1}H, ^{1}H-COSY and ^{1}H, ^{13}C-HMQC experiments. IR spectra were recorded in the region 4000–400 cm^{-1} on a Nicolet Avatar 360 FT IR spectrometer or a IFS66 Bruker spectrometer. The following compounds were synthesized according to literature procedures: Li(3,5-$Me_2C_5H_3BN$*i*-Pr_2),[11] Li($C_5H_4NMe_2$),[18] [AuCl(PPh_3)],[31] *trans*-[$PtCl_2$(CN*t*-Bu)$_2$][20] and *trans*-[$PtCl_2(NCPh)_2$].[19,32] The compound $C_5H_5NMe_2$ was obtained by reaction of $TsONMe_2$[33] with Na(C_5H_5)·DME,[34] which is a slight modification of the literature procedure in which methylsulfonyl chloride was reacted with Li(C_5H_5).[18]

Synthesis of Li[Mo(η^5-3,5-$Me_2C_5H_3BN$*i*-Pr_2)(CO)$_3$]·2 DME (Li·6·2DME). Solid [Mo(CO)$_6$] (3.98 g, 15.1 mmol) was added to a warm solution of Li(3,5-$Me_2C_5H_3BN$*i*-Pr_2) (3.18 g, 15.1 mmol) in DME (100 mL). The reaction mixture was stirred and heated to reflux temperature. It slowly turned yellow. After 24 h it was filtered through a frit covered with silica (4.5 cm layer) and further eluted with DME (3 × 10 mL). The volatiles were removed from the filtrate in vacuum. Pentane (50 mL) was then added to the residue. After stirring the mixture for 1 h the solid product was collected by filtration, washed with pentane (3 × 50 mL), and dried under vacuum to give Li·**6**·2DME (6.70 g, 78%) as a pale yellow solid; mp 102–103 °C, insoluble in pentane, soluble in toluene, DME and THF.

Data for Li·6·2DME. Anal. Calc. for $C_{24}H_{43}BLiMoNO_7$: C, 50.46; H, 7.59; N, 2.45. Found: C, 50.56; H, 7.10; N, 2.56%. ^{1}H NMR (THF-*d*$_8$): δ 4.69 (t, 1H, H-4), 3.81 (d, 2H, H-2/6, $^4J_{24} = 1.5$ Hz), 2.02 (s, 6H, Me-3/5); N*i*-Pr_2: 3.52 (sept, 2H, NCH), 1.17 (d, 12H, Me, $^3J = 6.8$ Hz; DME: 3.43 (s, 8H, CH_2), 3.27 (s, 12H, Me). ^{13}C{^{1}H} NMR (THF-*d*$_8$): δ 232.9 (CO), 125.1 (C-3/5), 84.3 (br, C-2/6), 81.0 (C-4), 25.7 (Me-3/5); N*i*-Pr_2: 46.0 (NCH), 22.8 (Me); DME: 72.6 (OCH_2), 58.7 (OMe). ^{11}B NMR (THF-*d*$_8$): δ 24.3. IR (KBr): *ν*(CO): 1916s, 1793s, 1747s cm^{-1}.

Synthesis of Li[Mo(η^5-$C_5H_4NMe_2$)(CO)$_3$]·2DME (Li·7·2DME). Solid [Mo(CO)$_6$] (2.87 g, 10.86 mmol) was added to a solution of Li($C_5H_4NMe_2$) (1.25 g, 10.86 mmol) in 100 mL dimethoxyethane (DME). The mixture was refluxed for 4 h with constant stirring. The disappearance of [Mo(CO)$_6$] was followed by IR spectroscopy. After concentration of the solution and precipitation with pentane (200 mL), the compound Li·**7**·2DME was isolated, washed with pentane (3 × 50 mL) and dried *in vacuo* to give a brown oil. The oil is very sensitive toward oxidation and should be kept at −30 °C. There are two moles of DME of solvation per mole of anion, this was determined by ^{1}H NMR spectroscopy. Yield 4.45 g, 86%.

Data for Li·7·2DME. ^{1}H NMR (($CD_3)_2CO$): AA′XX′ system δ 4.76 and 4.45 (2 pseudo-t, 8H, Cp), 3.48 (s, 8H, C*H*$_2$, DME), 3.30 (s, 12H, C*H*$_3$, DME), 2.34 (s, 6H, N(C*H*$_3$)$_2$). IR (THF): *ν*(CO): 1898s, 1799vs, 1773sh, 1709s cm^{-1}.

Synthesis of [Au{Mo(η^5-3,5-$Me_2C_5H_3BN$*i*-Pr_2)(CO)$_3$}(PPh_3)] (*Mo–Au*) (10). A mixture of [AuCl(PPh_3)] (0.60 g, 1.21 mmol) and Li·**6**·2DME (0.70 g, 1.23 mmol) in toluene (30 mL) was stirred for 2 h. The reaction mixture was then filtered through a frit covered with silica (9 cm layer). Concentration of the filtrate gave a viscous residue which was triturated with pentane to form a yellow suspension. The yellow solid was collected on a frit, washed with pentane (2 × 5 mL) and recrystallized from toluene to afford **10** (0.89 g, 87%); mp 171–172 °C.

*Data for **10**.* Anal. Calc. for $C_{34}H_{38}AuBMoNO_3P$: C, 48.42; H, 4.54; N, 1.66. Found: C, 48.76; H, 4.25; N, 1.98%. ^{1}H NMR (C_6D_6): δ 5.08 (br s, couplings not resolved, 1H, H-4), 4.58 (br s, coupling not resolved, 2H, H-2/6), 2.02 (s, 6H, Me-3/5); N*i*-Pr_2: 3.57 (sept, 2H, NCH), 1.25 (d, 12H, Me, $^3J = 6.8$ Hz); PPh_3: 7.5 (m, 6 H_o), 7.0 (m, 6 H_m + 3 H_p). ^{13}C{^{1}H} NMR (C_6D_6): δ 228.4 (CO), 127.1 (C-3/5), 86.4 (br, C-2/6), 84.2 (C-4), 25.7 (Me-3/5); N*i*-Pr_2: 46.2 (NCH), 22.7 (Me); PPh_3: 134.3 (d, $J_{PC} = 15$ Hz, C_o), 131.3 (d, $J_{PC} = 11$ Hz, C_m), 131.1 (d, $J_{PC} = 51$ Hz, C_i), 129.0 (d, $J_{PC} = 2$ Hz, C_p). ^{11}B NMR (C_6D_6): δ 24.7. IR (KBr): *ν*(CO): 1952s, 1862s, 1828s cm^{-1}.

Synthesis of [Hg{Mo(η^5-3,5-$Me_2C_5H_3BN$*i*-Pr_2)(CO)$_3$}Cl] (*Hg–Mo*) (11). Solid $HgCl_2$ (0.50 g, 1.84 mmol) was added to a suspension of Li·**6**·2DME (0.95 g, 1.66 mmol) in toluene (40 mL). After the mixture was stirred for 2 h, the resulting dark yellow suspension was filtered through a frit covered with silica (4 cm layer) and further eluted with toluene (2 × 20 mL) in order to achieve complete extraction. After removal of the volatiles the yellow residue was triturated and washed with pentane (5 × 3 mL). It was then recrystallized from a small amount of toluene at −30 °C to give, after drying under vacuum, **11** (0.88 g, 85%) as a bright yellow crystalline solid; mp 167–168 °C (decomp.), soluble in toluene and insoluble in pentane.

Anal. Calc. for $C_{16}H_{23}BClHgMoNO_3$: C, 30.99; H, 3.74; N, 2.26. Found: C, 30.89; H, 3.71; N, 2.18%. ^{1}H NMR (C_6D_6): δ 4.84 (br s, couplings not resolved, 1H, H-4), 4.18 (d, 2H, H-2/6, $^4J_{24} = 1.2$ Hz), 1.39 (s, 6H, Me-3/5); N*i*-Pr_2: 3.29 (sept, 2H, NCH), 1.18 and 1.11 (2d, 2 × 6 H, $^3J = 6.8$ Hz). ^{13}C{^{1}H} NMR (C_6D_6): δ 221.7 (CO), 123.3 (C-3/5), 85.9 (C-4), 84.7 (br, C-2/6), 23.7 (3-/5-Me); N*i*-Pr_2: 46.5 (NCH), 22.5 and 21.6 (Me). ^{11}B NMR (C_6D_6): δ 24.3. IR (KBr): *ν*(CO): 2020s, 1940s, 1922s cm^{-1}.

Synthesis of [Hg{Mo(η^5-3,5-Me$_2$C$_5$H$_3$BN*i*-Pr$_2$)(CO)$_3$}$_2$] (*Mo–Hg–Mo*) (12). A suspension of HgCl$_2$ (0.22 g, 0.83 mmol) and Li·**6**·2DME (0.96 g, 1.68 mmol) in toluene (80 mL) was stirred for 2 h. The reaction mixture was then filtered through a frit covered with silica (9 cm layer), and all volatiles were removed from the filtrate. The residue was washed with pentane and recrystallized from toluene to produce **12** (0.70 g, 87%) as a bright yellow solid; mp 260–262 °C.

*Data for **12***. Anal. Calc. for $C_{32}H_{46}B_2HgMo_2N_2O_6$: C, 39.67; H, 4.79; N, 2.89. Found: C, 39.88; H, 4.91; N, 2.98%. ^{1}H NMR (C_6D_6): δ 5.17 (br s, couplings not resolved), 1H, H-4), 4.31 (d, 2H, H-2/6, $^4J_{24} = 1.2$ Hz), 1.83 (s, 6H, Me-3/5); N*i*-Pr$_2$: 3.47 (sept, 2H, NCH), 1.19 (d, 12H, Me, ^3J = 6.8 Hz). ^{13}C{^{1}H} NMR (C_6D_6): δ 226.1 (CO), 126.2 (C-3/5), 87.3 (br, C-2/6), 85. 1 (C-4), 25.3 (Me-3/5); N–*i*Pr$_2$: 46.2 (NCH), 22.5 (br, Me). ^{11}B NMR (C_6D_6): δ 24.7. IR (KBr): *ν*(CO): 1962s, 1899br s cm^{-1}.

Synthesis of [Hg{Mo(η^5-C$_5$H$_4$NMe$_2$)(CO)$_3$}Cl] (15). Solid HgCl$_2$ (0.05 g, 0.17 mmol) was added to a suspension of Li·**7**·2DME (0.082 g, 0.17 mmol) in toluene (20 mL). After the mixture was stirred for 4 h, the resulting pale yellow suspension was filtered. After removal of the volatiles under reduced pressure, the pale yellow residue was washed with pentane (5 × 3 mL). It was then recrystallized by layering a toluene solution with pentane and storing at −30 °C. Complex **15** was isolated as pale yellow crystals. Their quality was only sufficient for a preliminary X-ray diffraction study. Yield: 0.035 g, 39%. IR (THF): *ν*(CO): 2001vs, 1967vs, 1915vs cm^{-1}. ^{1}H NMR (CDCl$_3$): AA′XX′ system δ 5.10 and 4.60 (2 pseudo-t, 8H, Cp), 2.59 (s, 12H, NMe$_2$).

Synthesis of *trans*-[Pt{Mo(η^5-C$_5$H$_4$NMe$_2$)(CO)$_3$}$_2$(CN*t*-Bu)$_2$] (*Mo–Pt–Mo*) (16). Solid *trans*-[PtCl$_2$(CN*t*-Bu)$_2$] (0.12 g, 0.28 mmol) was added to a stirred solution of Li·**7**·2DME (0.26 g, 0.56 mmol) in THF (20 mL) at −40 °C. Under constant stirring, the temperature was slowly raised to reach 20 °C in 8 h. The solution was filtered through Celite and most of the solvent was evaporated under reduced pressure. After addition of pentane and storing the mixture overnight in a freezer, the product precipitated as an orange powder. It was washed with water and ethanol and dried in vacuum. Orange-red crystals of **16** were obtained after recrystallization from THF–pentane. Yield: 0.18 g, 69%.

*Data for **16***. Anal. Calc. for $C_{30}H_{38}Mo_2N_4O_6Pt$: C, 38.43; H, 4.09; N, 5.98. Found: C, 37.86; H, 3.92; N, 5.67%. ^{1}H NMR (C_6D_6): AA′XX′ system δ 5.01 and 4.57 (2 pseudo-t, 8H, Cp), 2.24 (s, 12H, NMe$_2$), 1.23 (s, 18H, C*H*$_3$, *t*-Bu). ^{13}C{^{1}H} NMR (C_6D_6): δ 242.3 (CO), 84.7 and 74.6 (8C, *C*H from Cp), 40.9 (N(*C*H$_3$)$_2$), 29.5 (*C*H$_3$ from *t*-Bu). IR (KBr): *ν*(NC): 2168s, *ν*(CO): 1907vs, 1850vs br, 1830vs cm^{-1}.

Synthesis of *trans*-[Pt{Mo(η^5-C$_5$H$_4$NMe$_2$)(CO)$_3$}$_2$(NCPh)$_2$] (*Mo–Pt–Mo*) (17). Solid *trans*-[PtCl$_2$(NCPh)$_2$] (0.069 g, 0.15 mmol) was added to a stirred solution of Li·**7**·2DME (0.14 g, 0.29 mmol) in toluene (5 mL) at −40 °C. The reaction mixture was slowly brought to 20 °C in 8 h with constant stirring. The solution was filtered and the red–brown solid obtained was washed with toluene, water to remove the LiCl salt, and ethanol, affording the red–brown complex **17**. Owing to its poor solubility, no NMR data were obtained. Recrystallization from THF–pentane afforded orange crystals which readily desolvated in air. The crystal structure resolution indeed revealed the presence of two molecules of THF per mole of **17**. Yield: 0.08 g, 55%. The solution obtained after filtration of the toluene suspension was evaporated under reduced pressure. Extraction of the solid with pentane afforded the soluble complex [Mo(η^5-C$_5$H$_4$NMe$_2$)(CO)$_3$Cl] (**18**), which was characterized by X-ray crystallography. [IR (KBr): *ν*(CO): 2031vs, 1969vs, 1923vs cm^{-1}].

Table 2 Crystallographic data, data collection parameters and refinement results

	11	**16**	**17**·2THF	**18**	**20**
Formula	$C_{16}H_{23}BClHgMoNO_3$	$C_{30}H_{38}Mo_2N_4O_6Pt$	$C_{42}H_{46}Mo_2N_4O_8Pt$	$C_{10}H_{10}ClMoNO_3$	$C_{17}H_{15}ClMoN_2O_3Pt$
M_r	620.14	937.61	1121.80	323.58	621.79
Crystal system	Monoclinic	Monoclinic	Triclinic	Monoclinic	Triclinic
Space group	$P2_1/c$	$P2_1/c$	$P\bar{1}$	$P2_1/n$	$P\bar{1}$
a/Å	15.0320(12)	8.530(5)	8.518(5)	8.8250(3)	9.477(1)
b/Å	14.026(3)	17.111(5)	11.117(5)	10.7520(3)	9.637(1)
c/Å	19.843(2)	12.321(5)	12.785(5)	12.8080(4)	10.430(1)
α/°	90.00	90.00	94.91(5)	90.00	82.48(5)
β/°	107.908(8)	108.30(5)	109.36(5)	99.38(5)	83.48(5)
γ/°	90.00	90.00	107.20(5)	90.00	73.05(5)
V/Å^3	3981.0(10)	1707.3(13)	1068.3(9)	1199.07(6)	900.5(2)
Z	8	2	1	4	2
Crystal size/mm	0.32 × 0.07 × 0.04	0.10 × 0.10 × 0.10	0.10 × 0.10 × 0.10	0.10 × 0.10 × 0.10	0.10 × 0.10 × 0.10
Colour	Yellow	Orange	Orange	Orange	Orange
D_c/g cm^{-3}	2.069	1.824	1.744	1.792	2.293
μ/mm^{-1}	8.480	4.855	3.899	1.306	8.622
T/K	213(2)	173(2)	173(2)	173(2)	173(2)
F(000)	2352	912	552	640	584
Θ Limits/°	2.03/26.99	2.11/30.04	2.33/30.04	2.49/30.04	2.25/32.20
No. independent data	8648	4964	6094	3489	6234
No. data ($I > 2\sigma(I)$)	4197	3556	3564	2511	3771
No. parameters	446	196	259	145	226
R_1	0.0790	0.0332	0.0744	0.0383	0.0449
wR_2	0.0940	0.1098	0.1687	0.0865	0.1059
GOF	1.038	0.926	0.980	1.070	0.855
Max./min. $\Delta\rho$/e Å^{-3}	1.198/−1.311	1.130/−1.650	2.060/−1.443	1.033/−1.069	1.854/−1.846

Extraction of the residue with ether afforded an orange solution which was evaporated to dryness. Recrystallization from THF–pentane afforded a mixture containing the brown cluster $[\mathrm{Mo_2Pt_2}(\eta^5\text{-}\mathrm{C_5H_4NMe_2})_2(\mathrm{CO})_8]$ (**19**) (IR (KBr): *ν*(CO): 2029w, 1962vs, 1874vs cm^{-1}) and few crystals of the orange dimetallic complex $[\overline{\mathrm{Pt}\{\mathrm{Mo}(\eta^5\text{-}\mathrm{C_5H_4N}}\mathrm{Me_2})(\mathrm{CO})_3\}(\mathrm{NCPh})\mathrm{Cl}]$ (*Mo–Pt*) (**20**).

*Data for **17***. Anal. Calc. for $\mathrm{C_{34}H_{30}Mo_2N_4O_6Pt}$: C, 41.77; H, 3.09; N, 5.73. Found: C, 42.54; H, 3.16; N, 6.02%. IR (KBr): *ν*(CO): 1886s, 1846s, 1802s cm^{-1}.

Crystal structure determinations

The data collections were performed on an ENRAF-Nonius CAD4 diffractometer equipped with graphite monochromators using Mo-Kα radiation ($\lambda = 0.71073$ Å, ω–2θ scan) for complex **11** and on a Nonius Kappa-CCD area detector diffractometer (Mo-Kα, $\lambda = 0.71070$ Å, φ-scan) for compounds **16**, **17**·2THF, **18** and **20**. The relevant data are summarized in Table 2. The cell parameters were determined from reflections taken from one set of 10 frames (1.0° steps in φ angle), each at 20 s exposure. The structures were solved using direct methods (SHELXS97) and refined against F^2 using the SHELXL97 software. The absorption was corrected empirically (with Sortav) for the area detector data, whereas a numerical absorption correction was applied to the intensity data of **11**. All non-hydrogen atoms were refined with anisotropic parameters. The hydrogen atoms were included in their calculated positions and refined with a riding model in SHELXL97.

CCDC reference numbers 297952–297956.

For crystallographic data in CIF or other electronic format see DOI: 10.1039/b602106a

Acknowledgements

The work in Strasbourg was supported by the Ministry of Research (PhD grants to N. A. and P. C.), the CNRS and the Franco-German Research Training Group (GRK 532 of the DFG). The work in Aachen was generously supported by the Deutsche Forschungsgemeinschaft and the Fonds der Chemischen Industrie. One of us (T. S. B. B.) thanks North-Eastern Hill University, Shillong (India), for the grant of study leave. We are grateful to A. DeCian (Strasbourg) for the collection of the X-ray data and Dr R. Pattacini for help.

References

1 P. Braunstein, U. Englert, G. E. Herberich and M. Neuschütz, *Angew. Chem., Int. Ed. Engl.*, 1995, **34**, 1010.
2 R. Bender, P. Braunstein, J. M. Jud and Y. Dusausoy, *Inorg. Chem.*, 1983, **22**, 3394.
3 P. Braunstein, E. Cura and G. E. Herberich, *J. Chem. Soc., Dalton Trans.*, 2001, 1754.
4 G. Raabe, E. Heyne, W. Schleker and J. Fleischhauer, *Z. Naturforsch., Teil A*, 1984, **39**, 678.
5 G. Raabe, W. Schleker, E. Heyne and J. Fleischhauer, *Z. Naturforsch., Teil A*, 1987, **42**, 352.
6 G. E. Herberich, B. Schmidt, U. Englert and T. Wagner, *Organometallics*, 1993, **12**, 2891.
7 A. J. Ashe, III, J. W. Kampf, C. Mueller and M. Schneider, *Organometallics*, 1996, **15**, 387.
8 G. E. Herberich, G. Greiss and H. F. Heil, *Angew. Chem., Int. Ed. Engl.*, 1970, **9**, 805.
9 G. E. Herberich, B. Schmidt and U. Englert, *Organometallics*, 1995, **14**, 471.
10 G. E. Herberich, U. Englert, M. U. Schmidt and R. Standt, *Organometallics*, 1996, **15**, 2707.
11 B. Wang, X. Zheng and G. E. Herberich, *Eur. J. Inorg. Chem.*, 2002, 31.
12 J. Pethe, C. Maichle-Mossmer and J. Strähle, *Z. Anorg. Allg. Chem.*, 1997, **623**, 1413.
13 R. J. Haines, R. S. Nyholm and M. H. B. Stiddard, *J. Chem. Soc. A*, 1968, 46.
14 B. N. Strunin, K. I. Grandberg, V. G. Andrianov, V. N. Setkina, E. G. Perevalova, Y. T. Struchkov and D. N. Kursanov, *Dokl. Akad. Nauk SSSR*, 1985, **281**, 599.
15 M. J. Albright, M. D. Glick and J. P. Oliver, *J. Organomet. Chem.*, 1978, **161**, 221.
16 C. Bueno and M. R. Churchill, *Inorg. Chem.*, 1981, **20**, 2197.
17 F. H. Allen, O. Kennard, D. G. Watson, L. Brammer, A. G. Orpen and R. Taylor, *J. Chem. Soc., Perkin Trans. 2*, 1987, S1.
18 M. Bernheim and G. Boche, *Angew. Chem., Int. Ed. Engl.*, 1980, **92**, 1010.
19 P. Braunstein, R. Bender and J.-M. Jud, *Inorg. Synth.*, 1989, **26**, 341.
20 J. P. Barbier and P. Braunstein, *J. Chem. Res. (S)*, 1978, 412.
21 M. D. Curtis and W. M. Butler, *J. Organomet. Chem.*, 1978, **155**, 131.
22 R. Bender, P. Braunstein, J.-M. Jud and Y. Dusausoy, *Inorg. Chem.*, 1984, **23**, 4489.
23 P. Braunstein, E. Keller and H. Vahrenkamp, *J. Organomet. Chem.*, 1979, **165**, 233.
24 M. D. Curtis, K. R. Han and W. M. Butler, *Inorg. Chem.*, 1980, **19**, 2096.
25 R. J. Klingler, W. M. Butler and M. D. Curtis, *J. Am. Chem. Soc.*, 1978, **100**, 5034.
26 F. A. Cotton, L. Kruczynski and B. A. Frenz, *J. Organomet. Chem.*, 1978, **160**, 93.
27 (*a*) C. P. Casey, R. M. Bullock, W. C. Fultz and A. L. Rheingold, *Organometallics*, 1982, **1**, 1591; (*b*) C. P. Casey, R. M. Bullock and F. Nief, *J. Am. Chem. Soc.*, 1983, **105**, 7574; (*c*) C. Brumas, D. de Caro, F. Dehan, D. de Montauzon and R. Poilblanc, *Organometallics*, 1993, **12**, 1503; (*d*) L. Spadoni, C. Lo Sterzo, R. Crescenzi and G. Frachey, *Organometallics*, 1995, **14**, 3149.
28 F. Angelucci, A. Ricci, C. Lo Sterzo, D. Masi, C. Bianchini and G. Bocelli, *Organometallics*, 2002, **21**, 3001.
29 T. E. Bitterwolf, S. Gallagher, J. T. Bays, B. Scallorn, A. L. Rheingold, I. A. Guzei, L. Liable-Sands and J. C. Linehan, *J. Organomet. Chem.*, 1998, **557**, 77.
30 D. E. Crotty, E. R. Corey, T. J. Anderson, M. D. Glick and J. P. Oliver, *Inorg. Chem.*, 1977, **16**, 920.
31 P. Braunstein, H. Lehner and D. Matt, *Inorg. Synth.*, 1990, **27**, 218.
32 F. R. Hartley, *Organomet. Chem. Rev., Sect. A*, 1970, **6**, 119.
33 D. H. Barton, L. Bould, D. L. Clive, P. D. Magnus and T. Hase, *J. Chem. Soc., Perkin Trans. 1*, 1971, **12**, 2204.
34 M. Cheong and F. Basolo, *Organometallics*, 1988, **7**, 2041.